Available online at www.sciencedirect.com
ScienceDirect
Journal of Power Sources 164 (2007) 578–589
JOURNAL OF POWER SOURCES
www.elsevier.com/locate/jpowsour

Reduction of chromium vaporization from SOFC interconnectors by highly effective coatings

M. Stanislowski *, J. Froitzheim, L. Niewolak, W.J. Quadakkers, K. Hilpert, T. Markus, L. Singheiser

Research Center Juelich, Institute for Materials and Processes in Energy Systems (IWV-2), 52425 Jülich, Germany

Received 18 May 2006; received in revised form 29 June 2006; accepted 1 August 2006
Available online 4 December 2006

Abstract

The vaporization of Cr-rich volatile species from interconnector materials is a major source of degradation that limits the lifetime of planar SOFC systems with metallic interconnects. In this study, the vaporization of Cr species of a variety high chromium alloys was studied at 800 °C in air using the transpiration method. The measured release of Cr species of the different alloys was correlated with the formed outer oxide scales. A quantitative estimation showed that all the investigated alloys failed to meet the requirements concerning the Cr release from interconnector materials for SOFCs or formed oxide scales which possessed too high electrical resistances. Sputtered ceramic coatings of LSM and LSC and metallic coatings of Co, Ni and Cu were tested with regard to their suitability for Cr retention. The sputtered perovskite coatings turned out to be ineffective in reducing the Cr release to the desired levels. With metallic coatings of Co, Ni or Cu the Cr release could be reduced by more than 99%. The metallic coatings and their oxides effectively reduced the growth of the oxide scale on the steel substrate and showed negligible vaporization rates for Co, Cu and Ni, respectively. Therefore, Co, Ni or Cu were identified as promising and cheap coating materials for metallic interconnectors.

Keywords: Protective coatings; Chromium vaporization; Poisoning; Degradation

1. Introduction

Metallic interconnectors play a key role in the development of planar solid oxide fuel cells (SOFCs) [1]. They act as a physical separation between anode and cathode gases and provide the electronic connection between the single cells of the stack. The technical requirements for these materials comprise a high resistance against oxidation and creep at temperatures between 700 and 900 °C in oxidizing and reducing atmospheres, a high electrical conductivity of the surface oxide scales, gas tightness and a thermal expansion coefficient (CTE) similar to those of the electrolyte and the electrodes. Ferritic steels with chromium contents >20 wt.% and Cr based alloys were identified as the best suited materials for this purpose [2]. Commercial alloys of these type are, for example, the ferritic stainless steel E-Brite (Allegheny Ludlum, Pittsburgh, USA) or the Cr-based ODS-alloy Ducrolloy (Plansee AG, Reutte, Austria). At high temperatures these alloys form an oxide scale of Cr_2O_3 that protects the material from rapid oxidation while simultaneously retaining a comparatively high electrical conductivity.

During operation of planar SOFCs with metallic interconnects rapid degradations of the cell performance occurred which were caused by the release of gaseous Cr species from these materials, which is in the following designated as "Cr vaporization" [3–6]. The volatile Cr species are reduced at the triple phase points of cathode, electrolyte and air and form solid Cr_2O_3 and other Cr-rich phases [5,7,8] thereby inhibiting the electrochemical processes of the cell. This effect is often called "poisoning" of the cathode by gaseous Cr species. Corresponding degradation mechanisms were proposed by Hilpert et al. [9,10] and Jiang et al. [11,12].

It was further observed, that Cr_2O_3 and volatile Cr species may react with Ba-containing glass ceramic sealing materials thereby forming solid $BaCrO_4$ [13]. During long term service this can lead to an embrittlement of the sealing and to a deterioration of the gas tightness of the stack.

* Corresponding author. Tel.: +49 2461 615896; fax: +49 2461 613699.
E-mail address: m.stanislowski@fz-juelich.de (M. Stanislowski).

0378-7753/$ – see front matter © 2006 Elsevier B.V. All rights reserved.
doi:10.1016/j.jpowsour.2006.08.013

Different strategies were used to solve the problem of the Cr release from metallic interconnector materials and other SOFC components. They include a decrease of the operation temperature of the SOFC, the application of less Cr-sensitive cathode materials [6,14], the design of alternative multi-layer interconnects [15–17], the development of interconnect alloys with a lower Cr release and the use of Cr barrier coatings. Among these measures the last two are the most relevant in recent SOFC development.

It has been observed that the Cr vaporization can be reduced by the formation of outer spinel layers [2,18,19]. Generally, spinel phases possess comparatively high electronic conductivities which are for example utilized in electrical engineering for high-temperature conductors or NTC thermistors [20]. Based on this finding ferritic interconnect steels with defined contents of Mn, Ti and reactive elements (REs), such as Y, Ce, Zr or La, that form well-adherent outer (Cr,Mn)-spinel layers were developed recently. The most notable of these alloys are Crofer 22 APU (ThyssenKrupp VDM, Werdohl, Germany) [21], ZMG 232 (Hitachi Metals, Tokyo, Japan) [22] and the semi-commercial ODS-alloys IT-10, IT-11 and IT-14 (Plansee, Reutte, Austria) [23,24]. A number of studies of Cr vaporization of some of these steels is available (see e.g. [19,25]), however, only little is known about the actual Cr retention capability of $(Cr,Mn)_3O_4$ layers or other oxide scales. One aim of this work is to study systematically the Cr vaporization from alloys with different types of oxide layers on the outer surface.

For electrically insulating SOFC components alumina-forming alloys are sometimes considered. At high temperatures these alloys form slow-growing alumina scales at the surface that posses far better protective properties than chromia [2]. Due to the high electrical resistance of alumina these materials seem not suitable as construction materials for interconnectors [15]. Typical representatives of this material class are ferritic alloys of the Fecralloy type, that contain 15–23% Cr, 4.0–5.5% Al and 0.05–0.5% Y and/or other reactive elements [26]. The Cr release of alumina-forming alloys was investigated in a previous study [27].

Besides these efforts, coating systems were developed in order to reduce the Cr vaporization from stainless steels used as interconnectors [19,28–31]. They mostly consisted of perovskite layers on the basis of $(La,Sr)MnO_3$ [29,30,32,33], $(La,Sr)CoO_3$ [29,30,32–35], and $(La,Sr)CrO_3$ [19,36–39] or combinations of these [40]. Only few data are available on the Cr retention capabilities of these coatings (see e.g. [19]). There were also attempts with reactive coatings of La_2O_3 and SrO that form protective $(La,Sr)CrO_3$ layers in contact with Cr [38]. Due to the high inherent porosity the resulting Cr retention of these reactively formed layers was far below the expectations. More recently tests were performed with spinel coatings, especially of $(Co,Mn)_3O_4$ and $(Mn,Cr)_3O_4$ [41–44]. The results of Chen et al. [44] showed that Mn-Co-spinels are very promising coating materials with regard to suppresion of the sub-scale growth of Cr_2O_3 and increase of the electronic conductivity of the oxide scale. However, their actual Cr retention is unknown.

The most common coating techniques are vacuum plasma spraying (VPS) [19,29,45], wet powder spraying [38], slurry dip coating [46], and magnetron sputtering (MS) [34,36,37,39]. The aim of the second part of this study is to develop coating systems for reducing the Cr vaporization from stainless steels used as interconnectors and the increase of the electronic conductivity of the interconnector by reducing the growth of sublayered chromia scales.

2. Experimental

2.1. Alloys and coatings

The investigations were carried out with different Cr-based, Ni-based, and Co-based alloys, chromia-forming ferritic and austenitic steels and alumina-forming ferritic steels. The following alloys were selected for the experiments: Crofer 22 APU (batch KMT) (Mat. No. 1.4760, ThyssenKrupp VDM, Werdohl, Germany), E-Brite (UNS44627 Allegheny Ludlum, Pittsburgh, USA), Aluchrom YHf (Mat. No. 1.4767, ThyssenKrupp VDM, Werdohl, Germany), JS-3 (batch KDB) (Mannesmann Research Institute, Duisburg, Germany), IT-10 (batch KEX), IT-11 (batch KEZ), IT-14 (batch KGA), Ducrolloy (all Plansee AG, Reutte, Austria), Nicrofer 7520 (Mat. No. 2.4951), Nicrofer 45 TM (Mat. No. 2.4889), Nicrofer 6025 HT (Mat. No. 2.4633), Conicro 5010 W (Mat. No. 2.4964) (all ThyssenKrupp VDM, Werdohl, Germany) and Ferrotherm 4828 (Mat. No. 1.4828, ThyssenKrupp Schulte GmbH, Dortmund, Germany). The alloys contained different concentrations of alloying elements which are of importance for oxide scale formation, most notably Al, Si, Ti, Mn, Co, Ni, W, Mo and REs, such as (Y, La, Zr, Hf). The chemical compositions of the alloys determined by optical emission spectroscopy using an inductively coupled plasma (ICP-OES, IRIS-advantage, Thermo Jarrell Ash, Franklin, USA) are given in Table 1.

Various types of ceramic and metallic coatings were deposited by magnetron sputtering. For the ceramic coatings standard perovskite materials were selected which are used in SOFC technology as materials for ceramic interconnects and/or cathodes and which possess high electrical conductivities. These comprised the compositions $La_{0.8}Sr_{0.2}CrO_3$ (LSC-80, H.C. Starck GmbH, Goslar, Germany), $La_{0.99}(Cr_{0.77}Mg_{0.05}Al_{0.18})O_3$ (LMAC-DLR, DLR/Siemens, Stuttgart, Germany), $La_{0.80}Sr_{0.20}MnO_3$ (LSM-80, EMPA, Dübendorf, Switzerland) and $La_{0.65}Sr_{0.30}MnO_3$ (LSM-65, FZJ, Jülich, Germany). The electrical conductivities and the CTEs of these materials taken from the literature are given in Table 2. The sputtering targets were prepared from as-received powders by uniaxial pressing and subsequent sintering at 1400 °C for 5 h in air.

For the metallic coatings the transition metals Co (99.95% purity), Ni (99.99% purity) und Cu (99.99% purity) were selected. The sputtering targets were supplied by MaTeck GmbH, Jülich, Germany. The electrical conductivities and CTEs of these metals as well as their oxides from the literature are given in Table 2.

As substrate materials the ferritic steels Crofer 22 APU (KMT) and E-Brite were used. Before the sputtering the surfaces of the samples were ground with SiC-paper up to 1200 grit and cleaned in acetone and ethanol.

Table 1
Chemical compositions of the investigated alloys in wt.%, determined by ICP-OES

Grade	Fe	Cr	Ni	Co	Al	Si	Mn	Ti	Y	C	N	Others
Aluchrom YHf	74.7	20.2	0.18	–	**5.7**	0.3	0.2	–	**0.04**	0.024	0.005	**Hf: 0.04**
Conicro 5010 W	2.3	19.4	10.4	**48.9**	0.07	–	**1.5**	–	0.02	0.069	0.019	**W: 15.7**
Crofer 22 APU	76.5	22.7	0.02	–	0.02	0.02	**0.38**	**0.07**	–	0.002	0.004	**La: 0.06**
Ducrolloy	5.5	**92.9**	–	–	–	–	**–**	–	**0.48**	0.010	0.014	–
E-Brite	73.2	24.1	0.11	–	0.02	0.19	**0.04**	0.01	–	0.010	0.004	Mo: 0.96
Ferrotherm 4828	65.8	19.2	11.3	–	–	**1.7**	**1.3**	0.05	–	0.048	0.046	Mo: 0.96
IT-10	73.4	25.5	0.03	–	–	0.02	**N/A**	**N/A**	**0.07**	0.008	0.031	Mo: N/A
IT-11	71.8	26.4	0.03	–	0.02	0.01	**N/A**	**N/A**	**0.08**	0.009	0.020	Mo: N/A
IT-14	70.4	26.3	0.17	–	0.02	0.02	**N/A**	**N/A**	**0.06**	0.005	0.019	Mo: N/A
JS-3	76.1	22.7	–	–	0.02	–	**0.40**	**0.05**	–	0.016	–	**La: 0.09**
Nicrofer 45 TM	23.9	27.3	45.9	–	0.10	**2.7**	0.14	0.06	**0.08**	0.053	0.104	**Ce : 0.05**
Nicrofer 6025 HT	9.3	25.0	62.6	–	**2.30**	0.1	0.08	0.20	**0.08**	0.17	–	**La: 0.09**
Nicrofer 7520	4.00	19.3	75.4	–	0.12	0.5	**0.40**	**0.40**	–	0.09	0.005	–

The deposition of the coatings was performed by a magnetron-sputter facility (type Vacuum Classic 500 SP, Pfeiffer, Asslar, Germany). Before the sputtering process the surfaces of the samples were cleaned and roughened by pre-sputtering for 15 min at 250 W (RF) and an Ar pressure of 10^{-5} bar. The complete surfaces of the samples were coated by sputtering including the sides.

The ceramics were sputtered for 999 min at 100 W (RF). Thereby coating thicknesses of 32–45 μm were obtained. Co and Cu were sputtered at 200 W (DC) for 45 and 60 min, respectively. Ni was sputtered for 160 min at 100 W (DC). The resulting coatings had a thickness between 8 and 10 μm.

2.2. Vaporization measurements and characterization

The transpiration method was used for the measurement of the vaporization of chromium as well as manganese, cobalt, copper and nickel. The method is based on the principle that the volatile species formed over the heated sample are carried away by a constant gas flow and collected in a condenser. The masses of the transported elements are determined afterwards by quantitative chemical analysis. The gas flow rate has a significant effect on the vaporization rate. In the experiments the influence of the gas flow rate was eliminated by setting the gas flow to rates which were sufficiently high to ensure that the transported masses of Cr and Mn, Co, Cu and Ni depended solely on the kinetics of the vaporization reaction at the surface of the sample (see [25,57]).

The vaporization samples had dimensions of 80 mm × 20 mm and thicknesses between 1.5 and 3 mm. The edges of the samples were rounded by spark erosion in order to avoid starting points for oxide scale spallation during the vaporization experiments. Details on the geometry of the samples are given in [25]. The samples were ground with SiC paper up to 1200 grit and ultrasonically cleaned in ethanol and acetone.

The transpiration experiments were carried out with a constant flow of humidified air at 800 °C. The air flow was controlled by a flow meter, type 5850TR, supplied by Brooks, Veenendaal, The Netherlands. For the experiments the air flow rate was set to 1500 ml min^{-1}, referred to standard conditions (273 K,

Table 2
Literature data on thermal expansion coefficients (CTEs), α, and electrical conductivities, σ, of the used coating materials and their oxides

Name	$\alpha/10^{-6}$ K^{-1} (ΔT, °C)	σ (S cm^{-1}) T (°C)	Function
8YSZ	10.8(20–800) [47]	(5.3–4.5) × 10^{-2}(800) [48]	Electrolyte
Crofer 22 APU	12.0(20–800) [49]	8.70 × 10^3(800) [49]	Interconnect
Cr_2O_3	9.6(20–1400) [50]	1.28(750) [50] 2.50(1000) [50]	Oxide scale
$MnCr_2O_4$	7.2(25–900) [43]	0.22(750) [43] 0.05(800) [43]	Oxide scale
Mn_2CrO_4	–	12.8–30.3(750) [43]	Oxide scale
Co	14.0(20–400) [51]	1.71 × 10^4(800) [51]	Coating
Co_3O_4	–	35.5(800) [52]	Coating
$CoCr_2O_4$	7.4(25–900) [43]	1.92(750) [43]	Coating
Ni	16.3(20–900) [51]	2.20 × 10^4(900) [51]	Coating
NiO	12.6(100–800) [50]	14.9(590) [50] 71.4(1000) [50]	Coating
$NiCr_2O_4$	7.6(25–900) [43]	62.5(750) [43]	Coating
Cu	20.3(20–1000) [51]	1.23 × 10^5(977) [51]	Coating
CuO	–	2 × 10^3 (700) [50] 10^5(1000) [50]	Coating
LSC-80	9.8–11.2(20–1000) [53]	10–40(1000) [53]	Coating/interconnect
LMAC-DLR	–	–	Coating/interconnect
LSM-80	11.4(50–1000) [54]	175(1000) [55]	Coating/cathode
LSM-65	12.3(25–800) [47]	3.39(800) [56]	Coating/cathode

The values for other SOFC components are shown for comparison.

101,325 Pa). The humidity of the air was adjusted by a bubble humidifier and a condenser. The temperature of the condenser was controlled by a thermostat, type C10/K15, supplied by ThermoHaake, Karlsruhe, Germany. For the experiments, a water partial pressure of $p(H_2O) = 1.88 \times 10^3$ Pa was adjusted which corresponds to a relative humidity of 60% at 25 °C and standard air pressure. In order to ensure the saturation of the air with water vapour the bubble humidifier was heated to about 50 °C. After the experiments the condensate was dissolved in HCl (Merck, Suprapur®) and quantitatively analyzed by inductively coupled plasma mass spectrometry (ICP-MS, Perkin–Elmer, Norwalk, USA). Details on the experimental setup and the analysis are given in [58,25].

After the vaporization experiments, the samples were characterized by standard X-ray diffraction (XRD, X'Pert MRD, Philips, The Netherlands, Cu K_α radiation, 20–70°) and scanning electron microscopy (SEM, LEO 440 and LEO 1530–Gemini, Cambridge, UK) coupled with energy dispersive X-ray analysis (EDX, ISIS 300, Eynsham, UK).

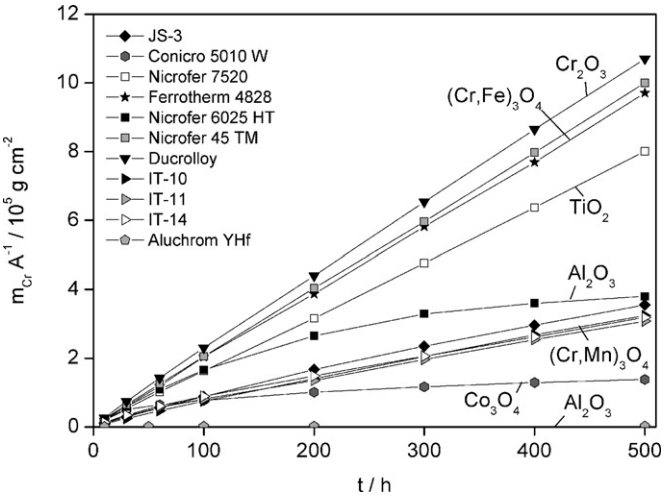

Fig. 1. Amount of released Cr per area as a function of time for the alloys, Ducrolloy, JS-3, IT-10, IT-11, IT-14, Nicrofer 7520, Nicrofer 45 TM, Nicrofer 6025 HT, Conicro 5010 W, Ferrotherm 4828, and Aluchrom YHf at 800 °C in air with $p(H_2O) = 1.88 \times 10^3$ Pa without pre-oxidation. The compositions of the outer oxide layers for the various alloys are indicated.

3. Results

3.1. Cr vaporization from alloys with different outer oxide scales

The vaporization experiments were carried out with non-preoxidized samples at 800 °C in air with a humidity of 1.88%. According to thermodynamic calculations with the program FactSage and the SGPS database $CrO_2(OH)_2(g)$ is under these conditions the most abundant volatile species of chromium, independent of the substrate material. Each sample was measured 8 times in succession up to a total time of 500 h. In order to obtain transported masses of Cr sufficiently large for reliable quantitative analysis by ICP-MS, the alloy Aluchrom YHf was measured only 5 times within 500 h. The results of the vaporization experiments are shown in Fig. 1 as total mass of vaporized Cr per unit area and time.

The type and thickness of the grown outer oxide scales on the samples, as well as the observed sublayers after the vaporization experiments at 800 °C for 500 h in air are given in Table 3.

3.2. Cr barrier coatings

Fig. 2 shows SEM images of sputtered perovskite coatings after the sputter process and after additional annealing treatments at 800 °C for 300 h in air. In order to improve the quality and the contrast of the cross-section images the surfaces of the samples were coated by a Au layer and a galvanic Ni layer before the final cross-section preparation for SEM analysis.

According to XRD analyses the perovskite layers were completely amorphous after sputtering. Full crystallization was observed after annealing at 800 °C for 10 h in air for all of the ceramic samples. The crystallized layers were all single-phase with exception of LSC-80 which contained small amounts of the secondary phase $SrCrO_4$ according to XRD. The XRD patterns of the coatings LSM-80 and LSM-65 showed minor amounts of Cr_2O_3 and $(Cr,Mn)_3O_4$ after oxidation at 800 °C for 10 h in air which was attributed to the oxidation of the substrate.

Table 3
Type and thickness of the outer oxide scales formed on the alloys, Ducrolloy, JS-3, IT-10, IT-11, IT-14, Nicrofer 7520, Nicrofer 45 TM, Nicrofer 6025 HT, Conicro 5010 W, Ferrotherm 4828, and Aluchrom YHf after oxidation of 500 h at 800 °C in air with 1.88% humidity

Alloy	Outer oxide layer	Thickness (μm)	Comment	Sublayer(s)
Aluchrom YHf	γ-/θ-Al_2O_3	0.6–1.9	Metastable	α-Al_2O_3
Conicro 5010 W	Co_3O_4	5.5	Gradient scale	$(Co,Cr)_3O_4$, Co_3W, Cr_2O_3
Crofer 22 APU	$(Mn,Cr)_3O_4$	0.7–1.3	Gradient scale	Cr_2O_3
Ducrolloy	Cr_2O_3	1.2	Pure scale	–
Ferrotherm 4828	$(Mn,Cr)_3O_4$	0.9–4.5	Poor adherence	Cr_2O_3
IT-10	$(Mn,Cr)_3O_4$	0.8–1.2	Gradient scale	Cr_2O_3
IT-11	$(Mn,Cr)_3O_4$	0.3	Gradient scale	Cr_2O_3
IT-14	$(Mn,Cr)_3O_4$	0.6–1.2	Gradient scale	Cr_2O_3
JS-3	$(Mn,Cr)_3O_4$	0.7–1.2	Gradient scale	Cr_2O_3
Nicrofer 45 TM	$(Cr,Fe)_3O_4$	1.3–3.3	Gradient scale	$(Cr,Fe)_2O_3$, SiO_2
Nicrofer 6025 HT	α-Al_2O_3	0.2–0.3	Slow growing	–
Nicrofer 7520	TiO_2	0.5–0.7	Low density	$(Cr,Fe)_3O_4$, Cr_2O_3

The observed sublayers as determined by SEM/EDX are also indicated.

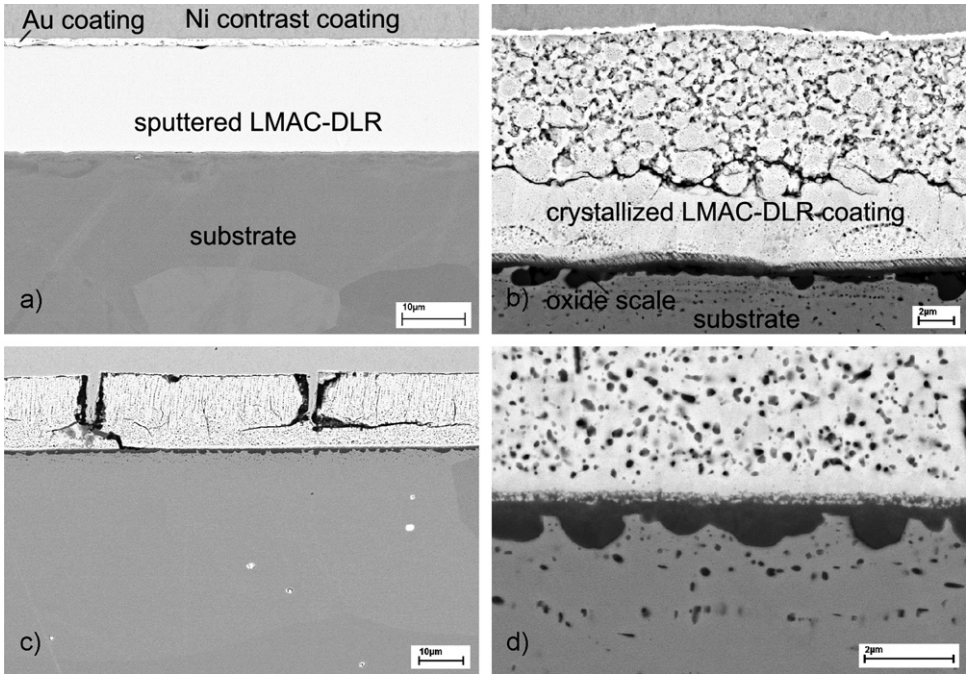

Fig. 2. SEM images of cross-sections of Crofer 22 APU (KMT) with coatings of (a) $La_{0.99}(Cr_{0.77}Mg_{0.05}Al_{0.18})O_3$ (LMAC-DLR) after sputtering; (b) sputtered LMAC-DLR after additional annealing at 800 °C for 300 h in humid air and 5 thermal cycles; and (c) and (d) $La_{0.80}Sr_{0.20}MnO_3$ (LSM-80) on Crofer 22 APU after annealing at 800 °C for 300 h in humid air.

Fig. 3 shows the Cr vaporization rates of Crofer 22 APU (KMT) with coatings of LSC-80, LMAC-DLR, LSM-65 and LSM-80 measured by the transpiration method. For comparison, the Cr vaporization rates of uncoated Crofer 22 APU (KMT) are also shown.

The coatings with LSM-65 and LSM-80 revealed extensive spallation after the first transpiration measurements. The vaporization experiments with LSC-80 coated samples were ceased after the first measurements as it was observed that the Cr retention was very low compared to the uncoated material.

Metallic coatings of Co, Cu and Ni on Crofer 22 APU and E-Brite were tested in the transpiration apparatus at 800 °C in air up to 1200 h. During the vaporization experiments the samples were heated up to 800 °C and cooled down to room temperature 3–4 times. Fig. 4 shows a SEM image of Crofer 22 APU with a sputtered coating of Co after oxidation at 800 °C for 1200 h in air. The distribution of the elements O, Co, Cr, Fe and Mn in the oxide scale are shown in separate maps.

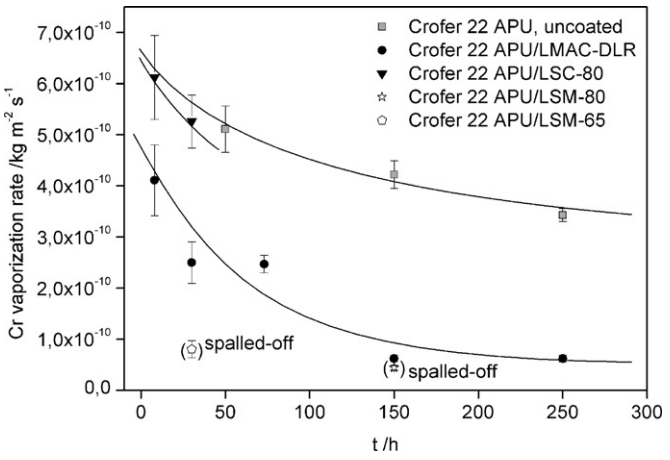

Fig. 3. Cr vaporization rates of Crofer 22 APU without coating and with sputtered coatings of $La_{0.8}Sr_{0.2}CrO_3$ (LSC-80), $La_{0.99}(Cr_{0.77}Mg_{0.05}Al_{0.18})O_3$ (LMAC-DLR), $La_{0.80}Sr_{0.20}MnO_3$ (LSM-80) and $La_{0.65}Sr_{0.30}MnO_3$ (LSM-65) at 800 °C in air with a humidity of $p(H_2O) = 1.88\%$.

Fig. 5 shows a SEM image and distribution maps of the elements O, Cu, Cr, Fe and Mn of Crofer 22 APU with a sputter coating of Cu after oxidation at 800 °C for 1200 h in humid air and 4 thermal cycles.

Fig. 6 shows a SEM image of Crofer 22 APU with a sputter coating of Ni after oxidation at 800 °C for 900 h in air and 3 thermal cycles. The distribution maps of the elements O, Co, Cr, Fe and Mn are also shown.

Fig. 7 shows the measured Cr vaporization rates of Crofer 22 APU with and without coatings of Co, Cu and Ni as a function of time at 800 °C in air with 1.88% humidity. The Cr vaporization rates of Co coatings on E-Brite are shown for comparison. Fig. 8 shows the vaporization rates of the coating elements Co, Cu and Ni under the same conditions.

4. Discussion

The results of the vaporization experiments in Fig. 1 show that the Cr retention of grown (Cr,Mn)-spinel layers on Cr_2O_3 scales, as in the case of JS-3, IT-10, IT-11 and IT-14, was about 60–70% compared to pure Cr_2O_3 scales, as in the case of Ducrolloy. The Cr vaporization of (Cr,Mn)-spinel-forming alloys was almost linear with time. A linear time dependence of the Cr vaporization was also observed for pure chromia scales and for Cr-rich spinel scales, as in the case of Ducrolloy

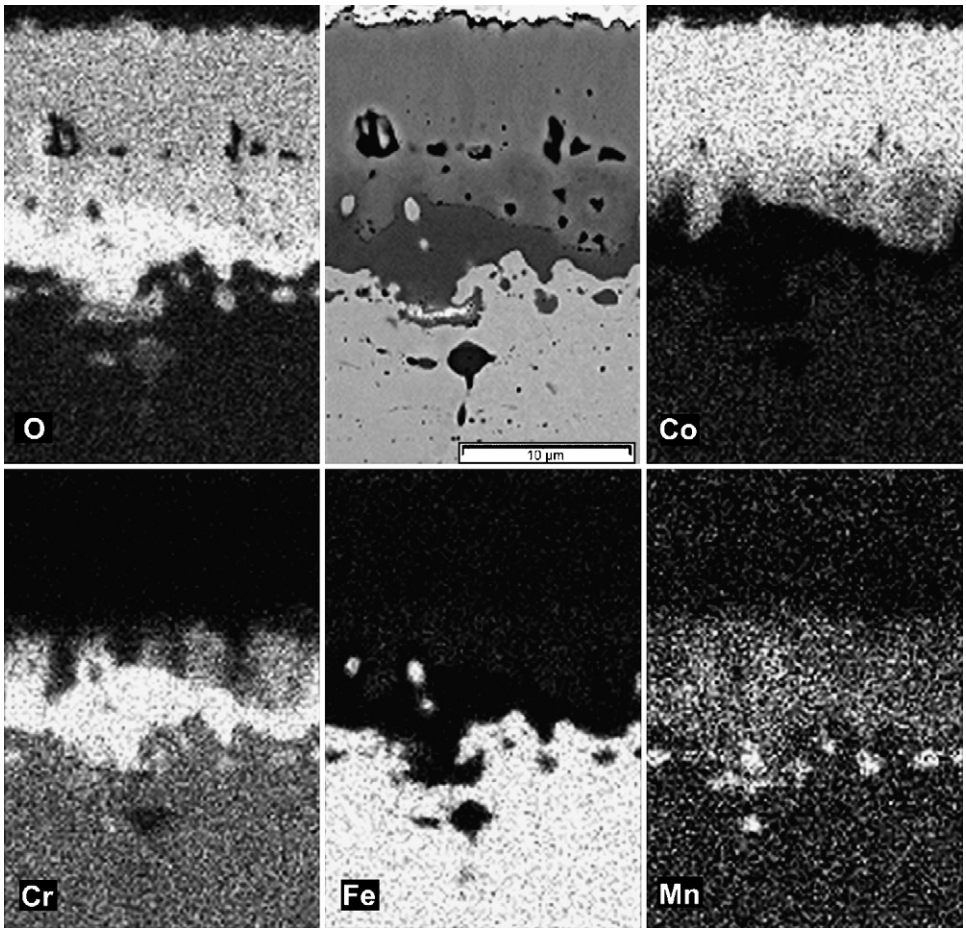

Fig. 4. SEM back scatter electron image of a sputtered Co layer on Crofer 22 APU (KMT) after oxidation at 800 °C for 1200 h in humid air and 4 thermal cycles. The distribution maps of the elements O, Co, Cr, Fe and Mn are also shown.

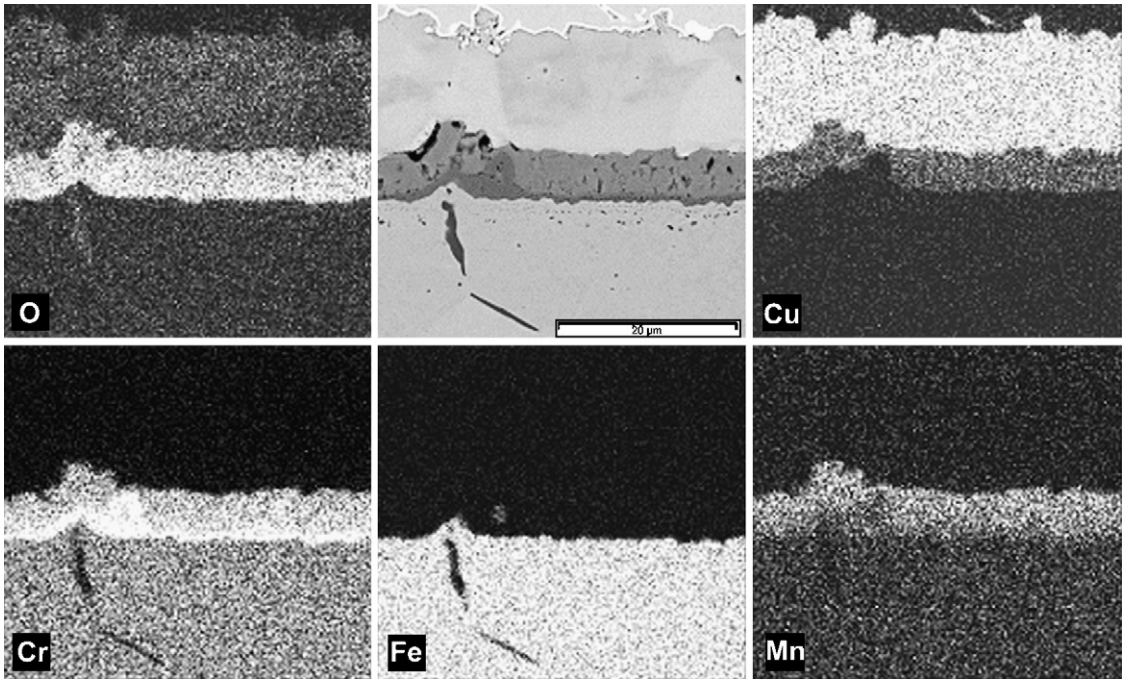

Fig. 5. SEM back scatter electron image of a sputtered Cu layer on Crofer 22 APU (KMT) next to distribution maps of the elements O, Cu, Cr, Fe and Mn after oxidation at 800 °C for 1200 h in humid air and 4 thermal cycles.

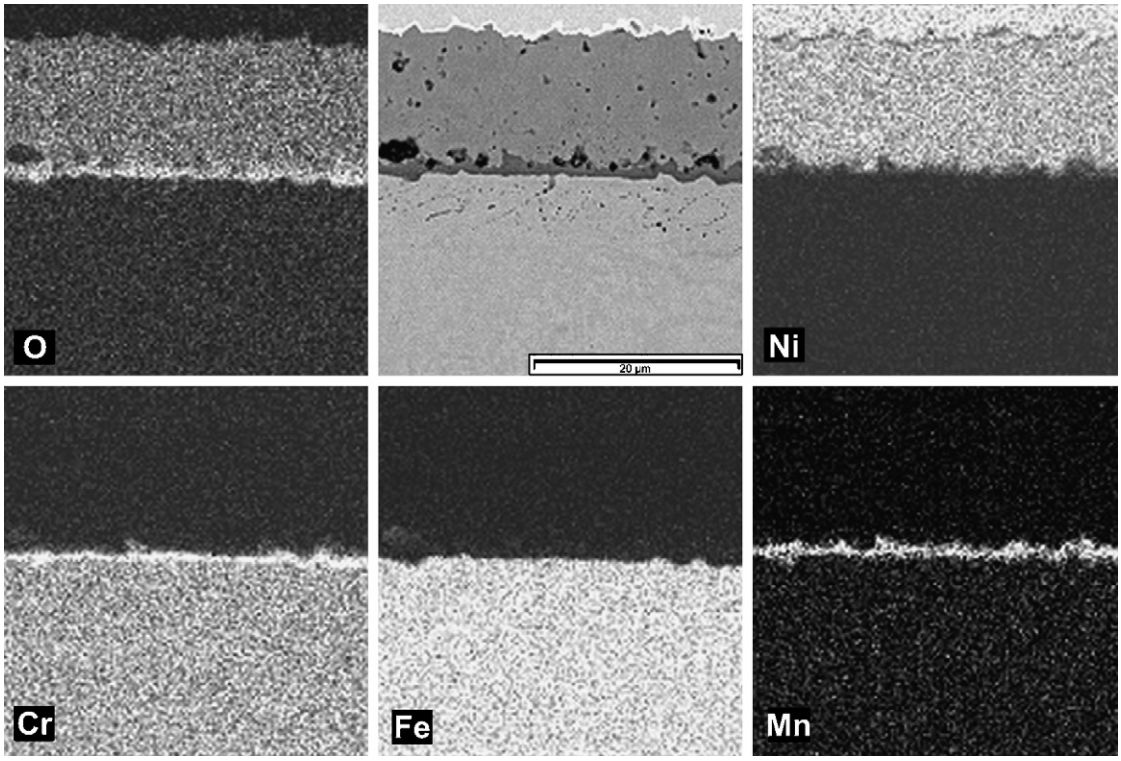

Fig. 6. SEM back scatter electron image of a sputtered Ni layer on Crofer 22 APU (KMT) next to distribution maps of the elements O, Ni, Cr, Fe and Mn after oxidation at 800 °C for 900 h in humid air and 3 thermal cycles.

and Nicrofer 45 TM, respectively. The vaporization kinetics in these cases are controlled by the vaporization reaction at the surface of the oxide scale. Different Cr vaporization kinetics are valid in the case of the alumina and cobalt oxide scales, from Nicrofer 6025 HT and Conicro 5010 W, respectively. These alloys showed a decrease of the Cr release with increasing time. The diffusion of Cr from the metal/oxide interface to the oxide surface seems to be the rate-determining step for the Cr vaporization in these two cases. From this it can be concluded that (Cr,Mn) spinel layers are not true barrier layers. The Cr vaporization from $(Cr,Mn)_3O_4$ layers is reduced due to the lower partial pressure of Cr over $(Cr,Mn)_3O_4$ compared to Cr_2O_3. This explains also the similar amounts of vaporized Cr per time and area from the different alloys JS-3, IT-10, IT-11 and IT-14 in spite of the different thicknesses of the formed spinel layers (see Table 3). The Cr transport through the Cr-Mn-spinel layer is fast and vaporized Cr can rapidly be replaced by diffusion. The fast diffusion is a result of the high defect concentration in the spinel

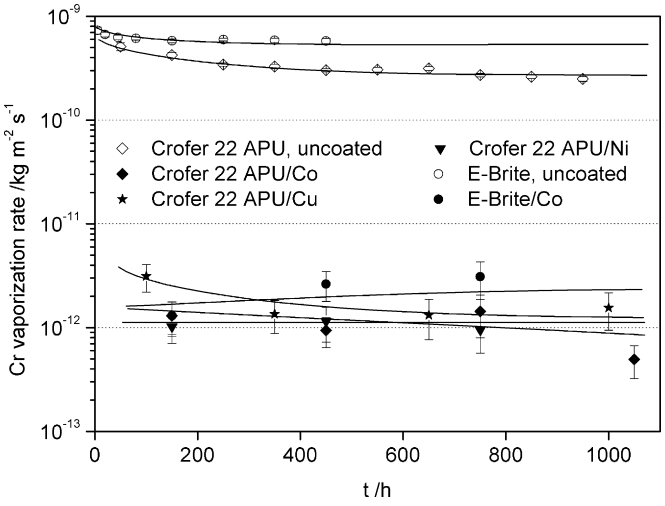

Fig. 7. Cr vaporization rates of Crofer 22 APU (KMT) with sputtered coatings of Co, Cu and Ni and without coating as a function of time at 800 °C in air with a humidity of $p(H_2O) = 1.88\%$. The Cr vaporization rates of E-Brite with and without Co coating are shown for comparison.

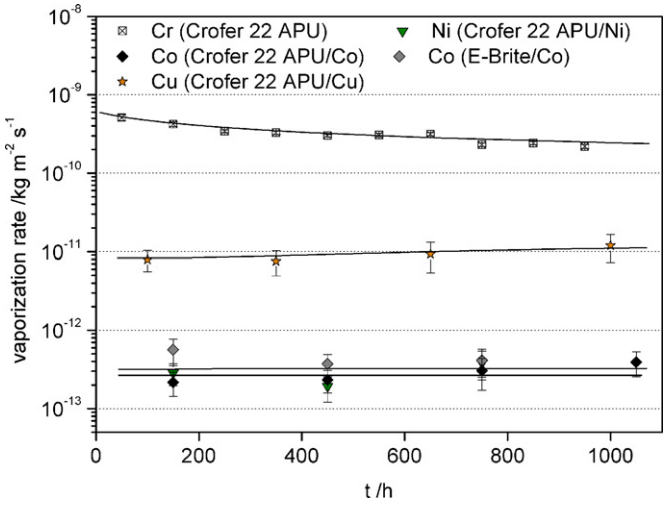

Fig. 8. Vaporization rates of the elements Co, Cu and Ni from sputtered Co, Cu and Ni coatings on Crofer 22 APU and E-Brite as a function of time at 800 °C in air with a humidity of $p(H_2O) = 1.88\%$. The Cr vaporization rates of uncoated Crofer 22 APU (KMT) are shown for comparison.

that becomes also evident by the large homegeinity region of the spinel phase in the phase diagram [59]. Due to this Al_2O_3 and Co_3O_4 are much more efficient Cr barrier layers. In the case of Co_3O_4, that was formed on Conicro 5010 W, the Cr retention was more than 90% compared to pure Cr_2O_3 after oxidation of 500 h at 800 °C in humid air. This finding, in combination with the fact that Co_3O_4 possesses a much higher electronic conductivity than Cr_2O_3 and $(Cr,Mn)_3O_4$ (see Table 2), makes Co_3O_4-forming alloys very interesting for application as SOFC interconnects. The potential of Co-based alloys as interconnector materials for SOFCs was identified by Kofstad and Bredesen [15]. However, the large thermal expansion mismatch between Co-based alloys (CTE Conicro 5010 W: $15.7 \times 10^{-6}\,K^{-1}$ from 20–800 °C [60]) and the electrolyte material YSZ (CTE 8YSZ: $10.8 \times 10^{-6}\,K^{-1}$ from 20–800 °C [47] and the high cost of Co are disadvantageous for the use of Co-based alloys as materials for SOFC interconnectors. Additionally, Co_3O_4-forming alloys exhibit high oxidation rates.

The best Cr retention capabilities were observed for alumina scales (Fig. 1). In the case of the Ni-based alloy, Nicrofer 6025 HT a very slow-growing alumina scale was formed. After oxidation of 500 h at 800 °C in humid air the alumina scale reached a thickness of just 200–300 nm and showed a Cr retention of about 90% compared to that of pure chromia. However, the formation of the alumina scale on Nicrofer 6025 HT turned out to be not fully reproducible and under certain conditions internal oxidation of Al beneath an outer chromia base scale was observed [27]. This can be explained by the relatively low Al content of Nicrofer 6025 HT. A rapid and reliable formation of alumina is obtained in the case of the ferritic alloy Aluchrom YHf. After about 100 h of oxidation at 800 °C in air the Cr release of this alloy was about 3 orders of magnitude lower than that of the chromia-forming alloy Ducrolloy. This corresponds to a Cr retention of more than 99.9%. As already mentioned, the high electrical resistance of alumina, which is about 5 orders of magnitude higher than that of to chromia [50], makes that alumina-forming alloys seemingly unsuitable as interconnect material.

Surface oxide layers of TiO_2, as in the case of Nicrofer 7520 turned out to be less effective as they were partially broken up and overgrown by Cr-Fe-spinel. This might be the result of the porosity and the uneven morphology of the underlying Fe–Cr oxide. Besides, the electrical conductivity of TiO_2 is highly uncertain, varying within 6 orders of magnitude between pure TiO_2 and oxygen-deficient $TiO_{2-\delta}$ [20].

The formation of Ni-containing oxide layers was not observed for any of the Ni-based alloys under the oxidation conditions at 800 °C in humid air.

The results in Fig. 1 give a good impression about the Cr retention capabilities and behaviour of different outer oxide scales on high chromium alloys. The question arises by which factor the Cr release of stainless steels used as interconnectors has to be decreased in order to achieve tolerable degradation rates and sufficient lifetimes of SOFC systems. Cell tests with uncoated (Cr,Mn)-spinel-forming alloys showed much too high degradation rates [6]. Tests at Research Center Juelich with cells using uncoated Crofer 22 APU as interconnector and $La_xSr_yMnO_3$ cathodes showed a performance degradation of about 21% after

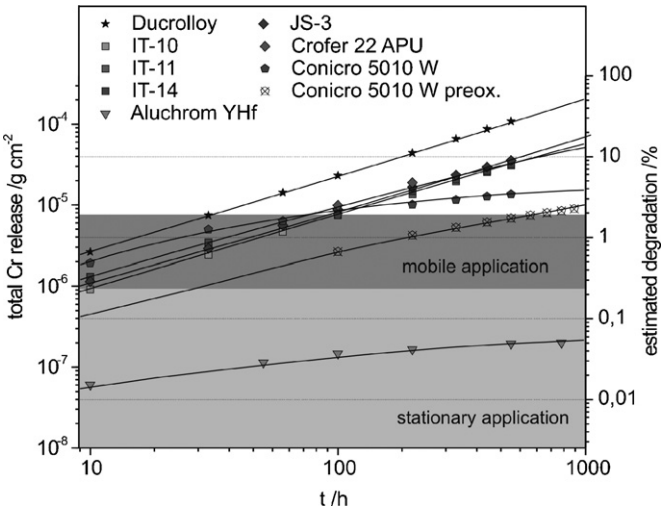

Fig. 9. Total amount of vaporized Cr per area as a function of time for non-oxidized Ducrolloy, IT-10, IT-11, IT-14, JS-3, Crofer 22 APU, Conicro 5010 W and Aluchrom YHf at 800 °C in air with 1.88% humidity. The estimated percentual degradation of the cell performance in combination with $La_xSr_yMnO_3$ cathodes for the application of these alloys as interconnector materials is shown on the right axis. The grey sectors mark tolerable degradation for stationary and mobile applications, respectively.

1000 h [61]. The degradation is mainly caused by Cr vaporization but other effects such as the growth of the oxide scale also play an important role. In order to estimate the degradation to be expected as a result of Cr vaporization from uncoated interconnector materials, the measured amounts of released Cr per time from Crofer 22 APU were compared with the empirical data from the cell tests with uncoated Crofer 22 APU as interconnectors. The measured degradation of the cell voltage was almost linear with time, a finding that was also reported by other authors [62]. It was assumed that the degradation of the cell was caused solely by Cr poisoning of the cathode. The Cr vaporization tests with uncoated alloys showed that after an oxidation time of about 100 h the Cr vaporization rates were nearly constant. Based on this it could be calculated that a Cr release of 3.96 $\mu g\,cm^{-2}$ in our measurements corresponded to a cell voltage degradation of 1% for the tested SOFC design at Research Center Juelich. This values were used to estimate the expected degradation effects of the other alloys investigated in this study from their measured Cr release values. The results are shown in Fig. 9. A realistic requirement for commercial SOFC systems is a performance degradation rate <2% per 1000 h for lifetimes of 5000–10,000 h for mobile applications and a performance degradation rate <0.25% per 1000 h for stationary applications with lifetimes of 40,000–100,000 h. Fig. 9 shows the total amount of vaporized Cr per area as function of time for the alloys Ducrolloy, IT-10, IT-11, IT-14, JS-3, Crofer 22 APU, Conicro 5010 W and Aluchrom YHf, and the expected degradation of the cell in percent. The targets mentioned above are marked by grey areas.

The curves in Fig. 9 are affected by different parameters including the flow rate, cathode material, humidity of the air, deviations in temperature, surface treatments and pre-oxidations of the stainless steels used as interconnectors. Therefore, slight shifts in the curves depending on the operation and design

of the SOFC system can occur. However, the diagram provides a reasonable estimate of the expected degradation of the different alloys relative to each other. From Fig. 9 it can be concluded that none of the tested alloys fulfils the requirements for SOFC interconnectors concerning the maximum Cr release per 1000 h. According to the estimation, the Cr release of $(Cr,Mn)_3O_4$-forming alloys is more than 10 times too high for mobile applications and more than 100 times too high for stationary applications. In the case of $(Cr,Mn)_3O_4$-forming alloys pre-oxidations have only minor effects as the Cr vaporization of these alloys is linear with time and independent of the thickness of the spinel layer (see text above). A pre-oxidation is useful in the case of Conicro 5010 W which forms a true Cr retention layer of Co_3O_4. This becomes obvious from Fig. 9 in which the calculated Cr vaporization of Conicro 5010 W is shown after a simulated pre-oxidation at 800 °C for 100 h in humid air. In this case the Cr release comes close to the limit for mobile applications. The results of Fig. 9 indicate, that the Cr vaporization of stainless steels cannot sufficiently be decreased by alloying solely.

Tests with ceramic coatings showed only moderate Cr retentions (see Fig. 3). The best results were obtained for a coating of LMAC-DLR, which decreased the Cr vaporization rates of Crofer 22 APU by a factor of 4–5. This is, however, far from the required decrease by at least a factor of 10 for mobile applications (see Fig. 9). The poor performance of perovskite coatings can be attributed to the high porosity that was observed for all of these samples. This is also the explanation for the significant oxidation of the substrates (Fig. 2) after 300 h of oxidation at 800 °C. The formation of pores can be considered as a result of the deposition by the sputter process. According to XRD data the coatings were fully amorphous after sputtering. Similar observations were reported by Johnson et al. and Orloskaya et al. [36,37]. During annealing at 800 °C crystallization took place. Thereby the density of the coating material changed which was accompanied by shrinkage and the formation of pores. Therefore, the occurrence of pores in the ceramic coating seems to be inherent to the sputter process. Porosity might be avoided to a certain extend by the use of alternative deposition techniques. Larring and Norby [40] reported that relatively dense perovskite coatings could be achieved by plasma spraying. Gindorf et al. [19] made vaporization tests with coatings of $La_{0.9}Sr_{0.1}CrO_3$ which were deposited on substrates of Ducrolloy by VPS. They observed a decrease of the Cr vaporization rates with increasing annealing times due to sintering effects in the coating. After several hundred hours exposure at 950 °C in air they measured Cr retentions of up to 99% compared to pure chromia scales. Tests in the present study with sputtered LMAC-DLR coatings which were sintered at 1000 °C for 100 h did not lead to an elimination of the pores. The manufacturing of dense perovskite coatings with sufficient Cr retention seems from this point of view to be complicated and expensive. The problems with porosity, the poor adherence of some of the perovskite coatings, especially of LSM, the comparatively low electronic conductivities (see Table 2), the inability to self healing or re-growth after spallation or damaging and the high material costs indicate that perovskites are not the material of choice for Cr barrier coatings on SOFC interconnectors.

The metallic Co, Cu and Ni coatings showed a reduction of the Cr release by more than 2 orders of magnitude compared to the uncoated substrate material Crofer 22 APU or by about 3 orders of magnitude compared to pure chromia scales at 800 °C in humid air (see Fig. 7). The full Cr retention was achieved from the beginning of the experiments. Even after 900 h or 1200 h of operation at 800 °C in humid air and 3–4 thermal cycles to room temperature no decrease of the Cr retention was observed. The results of Co-coated Crofer 22 APU and E-Brite show that the Mn content of the substrate alloy is not decisive for the Cr retention capability of the coating, as long as good adherence between steel and oxidized coating prevails. The SEM/EDX analyses in Figs. 4–6 showed, that the metallic coatings were completely oxidized during the annealing at 800 °C in humid air. According to XRD and EDX data the coatings consisted of Co_3O_4, CuO and NiO, respectively. The literature values of the electrical conductivities of these oxides are 1–2 orders of magnitude higher than that of Cr_2O_3 (see Table 2). The oxidized metallic coatings of Co, Cu and Ni formed effective barriers against oxidation of the substrate material. For the Co-coated sample the formed Cr-base oxide layer on the substrate had a thickness of 1.5–4.0 μm after 1200 h at 800 °C in humid air (see Fig. 4). Above the $Cr_2O_3/(Cr,Mn)_3O_4$ layer an interdiffusion zone consisting of Mn, Co and Cr spinels with a thickness of about 3 μm was observed. The oxide scale beneath the Cu coating had a thickness of about 6 μm after oxidation at 800 °C for 1200 h in humid air, and included a broad interdiffusion zone containing Cr, Mn and Cu (see Fig. 5). The higher oxidation of the substrate under the Cu coating can be explained by the high oxygen permeation of Cu or Cu-oxide. According to literature (see Table 2) the spinels formed in the interdiffusion zone can be expected to possess high electronic conductivities. In the case of the Ni coating the Cr-base oxide scale on the substrate reached a thickness of about 1 μm after oxidation at 800 °C for 900 h in humid air (see Fig. 6). Almost no interdiffusion of Ni and Cr/Mn was observed. According to Huczkowski et al. [63] the formed oxide scale on uncoated Crofer 22 APU depends on the thickness of the substrate. For substrates of 2 mm thickness as in the present study the oxide scale formed during oxidation at 800 °C for 1000 h in humid air reaches a thickness of about 2 μm. These results show that the oxidation of the substrate is reduced considerably by coatings of Co, Cu and especially of Ni. The coatings thereby help to reduce degradation effects of the cell performance caused by an increase of the cell resistance due to oxide scale growth, especially of chromia. The suppression of the oxide growth and the interdiffusion of the coating elements with the oxide scale on the substrate, especially in the case of the Co and Cu coatings, reduces the risk of scale spallation and provides an increase of the lifetime of the coating and the cell. It has to be verified by long term testing whether the external part of the initial layer of Cu, Ni or Cu remains a single phase oxide or whether it transforms into a Cr-containing spinel phase, which then might lead to an enhanced Cr vaporization.

In order to identify possible degradation effects caused by the coating materials the vaporization of Co, Cu and Ni was measured by the transpiration method (see Fig. 8). According to thermodynamic calculations with FactSage and the SGPS

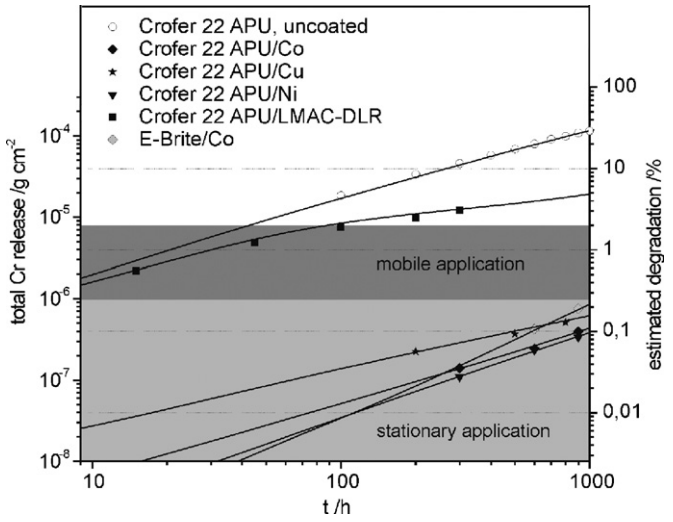

Fig. 10. Total amount of vaporized Cr per area as a function of time at 800 °C in air with 1.88% humidity for non-oxidized Crofer 22 APU (KMT) without coating and with coatings of LMAC-DLR, Co, Cu and Ni. The Cr release from Co-coated E-Brite is shown for comparison. The estimated percentual degradation of the cell performance in combination with $La_xSr_yMnO_3$ cathodes for the application of the coatings on interconnector materials is shown on the right axis. The grey sectors mark tolerable degradation for stationary and mobile applications.

data base [64] the formed species over Co_3O_4, CuO and NiO at 800 °C in humid air are $Cu(OH)_2$, Cu and $Ni(OH)_2$. The vaporization rates of Co and Ni from Co_3O_4 and NiO, respectively, are more than 2 orders of magnitude lower than the Cr vaporization from Crofer 22 APU and can most probably be neglected. In the case of CuO the vaporization rates of Cu are more than 1 order of magnitude lower than the Cr vaporization from Crofer 22 APU. Whether this might have a detrimental effect on the performance of the SOFC requires further investigations.

Fig. 10 shows a diagram similar to Fig. 9 in order to compare the Cr retention of the sputter coatings with the targets of SOFC development. It contains the estimated degradation caused by Co, Cu, Ni and LMAC-DLR coated Crofer 22 APU and E-Brite steel.

Fig. 10 shows that the metallic coatings of Co, Cu and Ni are suitable as Cr retention layers for SOFC interconnects, for mobile as well as for stationary application, independent of the substrate material. The perovskite type materials failed to reach the required reduction of the Cr release, which is mainly attributed to the high concentration of pores in the ceramic coatings. The excellent Cr retention, the stability at high temperature under oxidizing conditions, the effective decrease of substrate oxidation, the low costs and the possibility to be deposited by simple, rapid and cheap techniques, such as galvanization or metal plating makes metallic coatings of Co, Cu and Ni very promising for application on SOFC interconnectors.

5. Conclusion

The Cr vaporization of high chromium alloys with different outer oxide scales was systematically investigated at 800 °C. The chromium retention capability of steels which form a layer of Cr-Mn-spinel on top of a chromia scale was about 60–70%, compared to pure chromia-forming alloys. The differences concerning the Cr vaporization of different grades of these Cr-Mn-spinel-forming steels, such as Crofer 22 APU, IT-10, IT-11 or IT-14, were small and hardly depended on the thickness of the spinel layer. A reduction of the Cr release of about 90% was observed for Co-based alloys that formed an outer layer of Co_3O_4. The lowest Cr vaporizations were found for alumina forming steels, which also revealed the lowest electronic conductivity. An estimation of the degradation rates of the cell voltage as a consequence of the Cr vaporization from different uncoated interconnector alloys showed that all of the considered alloys failed to cope with the required maximum tolerable degradation rates of stationary and mobile SOFC systems.

Tests with sputtered ceramic Cr barrier coatings of $La_{0.8}Sr_{0.2}CrO_3$ (LSC-80), $La_{0.99}(Cr_{0.77}Mg_{0.05}Al_{0.18})O_3$ (LMAC-DLR), $La_{0.80}Sr_{0.20}MnO_3$ (LSM-80) and $La_{0.65}Sr_{0.30}MnO_3$ (LSM-65) on substrates of Crofer 22 APU showed only a minor reduction of the Cr release. This can mainly be explained by the formation of pores due to crystallization of the amorphous sputter coatings during high temperatures exposure. The LSM coatings showed a high tendency to spallation after thermal cycling which might be improved by a proper adjustment of the fabrication parameters, such as the thickness of the coating. It also has to be proven whether better results can be achieved by other deposition techniques, e.g. vacuum plasma spraying or dip coating. In general the application of perovskite Cr retention layers seems to be questionable due to high costs, comparatively low electronic conductivities and difficulties with the fabrication of dense coatings.

Metallic coatings of Co, Cu and Ni on Crofer 22 APU with a thickness of about 10 μm showed Cr retentions of more than 99% up to maximum test times of 1200 h at 800 °C in humid air. Vaporization tests with Co coatings on E-Brite showed similar results. From this it can be concluded that the coatings are effective for a wide range of stainless steels. These coatings fulfil the requirements for mobile and stationary long-term applications. The vaporization of Co, Ni and Cu at 800 °C in humid air is low and at least in case of Co and Ni negligible. The metallic coatings were completely oxidized to Co_3O_4, CuO and NiO, respectively, and showed good stability and adherence to the substrate up to annealing times of 1200 h at 800 °C. They significantly reduced the oxidation of the substrate and possess electronic conductivities which are 1–2 orders of magnitude larger than that of Cr_2O_3, according to literature. Coatings of Co, Cu and Ni or their oxides, Co_3O_4, CuO and NiO, respectively, provide high electronic conductivities for the interconnector and a decreased long-term degradation of the performance of the cell. Advantages of metallic Co, Ni or Cu coatings are their low costs and easy and rapid fabrication by a wide range of techniques, e.g. galvanization and plating. Metallic coatings of Co, Cu and Ni are therefore considered as interesting and promising coating materials for metallic SOFC interconnects. However, it has to be proven in further tests whether the electronic conductivites and long-term stabilities of the metallic coatings, also in combination with the cathode materials, are superior to other coating materials such as spinels or perovskites. The results of these tests

will also show which of the investigated metallic coatings, Co, Ni or Cu, is best suited for SOFC interconnectors.

Acknowledgements

The authors are grateful to their colleagues at Research Center Juelich for their assistance in doing this work, especially to Mr. P. Lersch (IWV-2) for performing the XRD measurements. ThyssenKrupp VDM, Werdohl (Germany), Plansee AG, Reutte (Austria), and Allegheny Ludlum, Pittsburgh (USA) are acknowledged for providing materials.

References

[1] F. Tietz, Mater. Sci. Forum 426–432 (2003) 4465–4470.
[2] W.J. Quadakkers, J. Piron-Abellan, V. Shemet, L. Singheiser, Mater. High Temp. 20 (2003) 115–127.
[3] S. Taniguchi, M. Kadowaki, H. Kawamura, T. Yasuo, Y. Akiyama, Y. Miyake, T. Saitoh, J. Power Sources 55 (1995) 73–79.
[4] S.P.S. Badwal, R. Deller, K. Föger, Y. Ramprakash, J.P. Zhang, Solid State Ionics 99 (1997) 297–310.
[5] Y. Matsuzaki, I. Yasuda, Solid State Ionics 132 (2000) 271–278.
[6] S.P. Simner, M.D. Anderson, G.-G. Xia, Z. Yang, L.R. Pederson, J.W. Stevenson, J. Electrochem. Soc. 152 (2005) A740–A745.
[7] S.C. Paulson, in: S.C. Singhal, M. Dokiya (Eds.), Proceedings of the 8th International Symposium on Solid Oxide Fuel Cells VIII (SOFC-VIII), proc. vol. 2003–07, Paris, France, April 27–May 02, 2003, p. 498.
[8] S.C. Paulson, V.I. Birss, J. Electrochem. Soc. 151 (2004) A1961–A1968.
[9] D. Das, M. Miller, H. Nickel, K. Hilpert, in: U. Bossel (Ed.), Proceedings of the 1st European Solid Oxide Fuel Cell Forum, Lucerne, Switzerland, October 3–7, 1994, p. 703.
[10] K. Hilpert, D. Das, M. Miller, D.H. Peck, R. Weiß, J. Electrochem. Soc. 143 (1996) 3642–3647.
[11] S.P. Jiang, J.P. Zhang, L. Apateanu, K. Foger, J. Electrochem. Soc. 147 (2000) 4013–4022.
[12] S.P. Jiang, S. Zhang, Y.D. Zhen, J. Mater. Res. 20 (2005) 747–758.
[13] Z.G. Yang, J.W. Stevenson, K.D. Meinhardt, Solid State Ionics 160 (2003) 213–225.
[14] T. Komatsu, H. Arai, R. Chiba, K. Nozawa, M. Arakawa, K. Sato, Electrochem. Solid State Lett. 9 (2006) A9–A12.
[15] P. Kofstad, R. Bredesen, Solid State Ionics 52 (1992) 69–75.
[16] W.A. Meulenberg, A. Gil, E. Wessel, H.P. Buchkremer, D. Stöver, Oxid. Met. 57 (2002) 1–12.
[17] W. Huang, S. Gopalan, Solid State Ionics 177 (2006) 347–350.
[18] J. Piron-Abellan, V. Shemet, F. Tietz, L. Singheiser, W.J. Quadakkers, in: H. Yokokawa, S.C. Singhal (Eds.), Proceedings of the 7th International Symposium on Solid Oxide Fuel Cells VII (SOFC-VII), proc. vol. 2001-16, Tsukuba, Japan, June 3–8, 2001, p. 811.
[19] C. Gindorf, L. Singheiser, K. Hilpert, Steel Res. 72 (2001) 528–533.
[20] H. Schaumburg, Werkstoffe und Bauelemente der Elektrotechnik Keramik, B.G. Teubner Verlag, Stuttgart, 1994.
[21] W.J. Quadakkers, V. Shemet, L. Singheiser, Patent DE 100 25 108 A1 (2000).
[22] T. Horita, Y. Xiong, K. Yamaji, N. Sakai, H. Yokokawa, J. Electrochem. Soc. 150 (2003) A243–A248.
[23] W. Glatz, M. Janousek, K. Honegger, Patent AT 4442001 (2001).
[24] W. Glatz, G. Kunschert, M. Janousek, in: M. Mogensen (Ed.), Proceedings of the 6th European Solid Oxide Fuel Cell Forum, Lucerne, Switzerland, June 28–July 2, 2004, p. 1612.
[25] M. Stanislowski, E. Wessel, K. Hilpert, T. Markus, L. Singheiser, J. Electrochem. Soc., in press.
[26] Z. Yang, K.S. Weil, D.M. Paxton, J.W. Stevenson, J. Electrochem. Soc. 150 (2003) A1188–A1201.
[27] M. Stanislowski, E. Wessel, K. Hilpert, T. Markus, L. Singheiser, J. Electrochem. Soc., submitted for publication.
[28] J. Urbanek, M. Miller, H. Schmidt, K. Hilpert, in: B. Thorstensen (Ed.), Proceedings of the 2nd European Solid Oxide Fuel Cell Forum, Oslo, Norway, May 6–10, 1996, p. 503.
[29] W.J. Quadakkers, H. Greiner, M. Hänsel, A. Pattanaik, A.S. Khanna, W. Mallener, Solid State Ionics 91 (1996) 55–67.
[30] E. Batawi, K. Honegger, R. Diethelm, M. Wettstein, in: B. Thorstensen (Ed.), Proceedings of the 2nd European Solid Oxide Fuel Cell Forum, Oslo, Norway, May 6–10, 1996, p. 307.
[31] P.Y. Hou, K. Huang, W.T. Bakker, in: S.C. Singhal, M. Dokiya (Eds.), Proceedings of the 6th International Symposium on Solid Oxide Fuel Cells VI (SOFC-VI), proc. vol. 99-19, Honolulu, Hawaii, USA, October 17–22, 1999, p. 737.
[32] E. Batawi, A. Plas, W. Straub, K. Honegger, R. Diethelm, in: S.C. Singhal, M. Dokiya (Eds.), Proceedings of the 6th International Symposium on Solid Oxide Fuel Cells VI (SOFC-VI), proc. vol. 99-19, Honolulu, Hawaii, USA, October 17–22, 1999, p. 767.
[33] H. Schmidt, B. Brückner, K. Fischer, in: M. Dokiya, O. Yamamoto, H. Tagawa, S.C. Singhal (Eds.), Proceedings of the 4th International Symposium on Solid Oxide Fuel Cells IV (SOFC-IV), proc. vol. 95-01, Yokohama, Japan, June 18–23, 1995, p. 869.
[34] D.O. Klenov, W. Donner, L. Chen, A.J. Jacobsen, S. Stemmer, J. Mater. Res. 18 (2003) 188–194.
[35] K. Fujita, K. Ogasawara, Y. Matsuzaki, T. Sakurai, J. Power Sources 131 (2004) 261–269.
[36] C. Johnson, R. Gemmen, N. Orlovskaya, Composites Part B 35 (2004) 167–172.
[37] N. Orolvskaya, A. Coratolo, C. Johnson, R. Gemmen, J. Am. Ceram. Soc. 87 (2004) 1981–1987.
[38] S. Linderoth, Surf. Coat. Technol. 80 (1996) 185–189.
[39] J.H. Zhu, Y. Zhang, A. Basu, Z.G. Lu, M. Paranthaman, D.F. Lee, E.A. Payzant, Surf. Coat. Technol. 177–178 (2004) 65–72.
[40] Y. Larring, T. Norby, J. Electrochem. Soc. 147 (2000) 3251–3256.
[41] Z. Yang, G. Xia, J.W. Stevenson, Electrochem. Solid-State Lett. 8 (2005) A168–A170.
[42] Z. Yang, G. Xia, S.P. Simner, J.W. Stevenson, J. Electrochem. Soc. 152 (2005) A1896–A1901.
[43] W. Qu, L. Jian, J.M. Hill, D.G. Ivey, J. Power Sources 153 (2006) 114–124.
[44] X. Chen, P.Y. Hou, C.P. Jacobson, S.J. Visco, L.C. De Jonghe, Solid State Ionics 176 (2005) 425–433.
[45] G. Schiller, R. Henne, R. Ruckdäschel, J. Adv. Mater. 32 (2000) 3–8.
[46] J.-H. Kim, R.-H. Song, S.-H. Hyun, Solid State Ionics 174 (2004) 185–191.
[47] D. Stöver, U. Diekmann, U. Flesch, H. Kabs, W.J. Quadakkers, F. Tietz, I.C. Vinke, in: S.C. Singhal, M. Dokiya (Eds.), Proceedings of the 6th International Symposium on Solid Oxide Fuel Cells VI (SOFC-VI), proc. vol. 99-19, Honolulu, Hawaii, USA, October 17–22, 1999, p. 812.
[48] T. Norby, P.A. Osborg, H. Raeder, in: B. Thorstensen (Ed.), Proceedings of the 2nd European Solid Oxide Fuel Cell Forum, Oslo, Norway, May 6–10, 1996, p. 315.
[49] ThyssenKrupp VDM, Material Data Sheet No. 8005, Edition June 2004.
[50] G.V. Samsonov, The Oxide Handbook, IFI/Plenum Data Company, New York, 1982.
[51] E.A. Brandes, Smithells Metals Reference Book, sixth ed., Butterworths, London, 1983.
[52] S. Sakamoto, M. Yoshinaka, K. Horita, O. Yamaguchi, J. Am. Ceram. Soc. 80 (1997) 267–268.
[53] J.W. Fergus, Solid State Ionics 171 (2004) 1–15.
[54] M. Mori, Y. Hiei, N.M. Sammes, G.A. Tompsett, in: S.C. Singhal, M. Dokiya (Eds.), Proceedings of the 6th International Symposium on Solid Oxide Fuel Cells VI (SOFC-VI), proc. vol. 99-19, Honolulu, Hawaii, USA, October 17–22, 1999, p. 347.
[55] S. Hashimoto, T. Shimura, H. Iwahara, in: S.C. Singhal, M. Dokiya (Eds.), Proceedings of the 6th International Symposium on Solid Oxide Fuel Cells VI (SOFC-VI), proc. vol. 99-19, Honolulu, Hawaii, USA, October, 17–22, 1999, p. 379.
[56] C.-C.T. Yang, W.-C.J. Wei, A. Roosen, Mater. Chem. Phys. 81 (2003) 134–142.

[57] H.K. Hofmeister, R.v. Haeseler, O. Glemser, Z. Elektrochem. 64 (1960) 513–517.
[58] M. Stanislowski, U. Seeling, D.-H. Peck, S.-K. Woo, L. Singheiser, K. Hilpert, Solid State Ionics 176 (2005) 2523–2533.
[59] D.H. Speidel, A. Muan, J. Ceram. Soc. 46 (1963) 577–578.
[60] Krupp VDM, Material Data Sheet No. 6002, Edition May 1994.
[61] I.C. Vinke, private communication, IWV-3, Research Centre Jülich, 2005.
[62] S.P.S. Badwal, R. Bolden, K. Föger, in: P. Stevens (Ed.), Proceedings of the 3rd European Solid Oxide Fuel Cell Forum, Nantes, France, 2–5 June, 1998, p. 105.
[63] P. Huczkowski, N. Christiansen, V. Shemet, J. Piron-Abellan, L. Singheiser, W.J. Quadakkers, Mater. Corros. 55 (2004) 825–830.
[64] G.W. Bale, A.D. Pelton, W.T. Thompson, G. Erikson, K. Hack, P. Chartrand, S. Degterov, J. Melançon, S. Petersen, FactSage v. 5.2, Thermfact, Montreal, Canada, 2001.